International Journal of Technology (2011) 1: 74-83
ISSN 2086-9614

COMPARISON OF PARTICLE SWARM OPTIMIZATION AND GENETIC ALGORITHM FOR MOLTEN POOL DETECTION IN FIXED ALUMINUM PIPE WELDING

Ario Sunar Baskoro [1*], Rui Masuda[2], Yasuo Suga[3]

[1]*Laboratory of Manufacturing Technology and Automation, Department of Mechanical Engineering, Faculty of Engineering, University of Indonesia, Kampus Baru UI Depok 16424 – Indonesia*
[2]*Graduate School of Science and Technology, Keio University*
[3]*Faculty of Science and Technology, Keio University*
3-14-1 Hiyoshi, Kohoku-ku, Yokohama 223-8522, Japan

(Received: December 2010 / Revised: December 2010 / Accepted: January 2011)

ABSTRACT
This paper proposes a study on the comparison of particle swarm optimization with genetic algorithm for molten pool detection in fixed aluminum pipe welding. The research was conducted for welding of aluminum alloy Al6063S-T6 with a controlled welding speed and a Charge-couple Device (CCD) camera as vision sensor. Omnivision-based monitoring using a hyperboloidal mirror was used to detect the molten pool. In this paper, we propose an optimized brightness range for detecting the molten pool edge using particle swarm optimization and compare the results to genetic algorithm. The values of the brightness range were applied to the real time control system using fuzzy inference system. Both optimization methods showed good results on the edge detection of the molten pool. The results of experiments with control show the effectiveness of the image processing algorithm and control process.

Keywords: Fixed aluminum pipe welding; Fuzzy inference system; Genetic algorithm; Molten pool detection; particle swarm optimization

1. INTRODUCTION
Recently, the arc welding process of aluminum alloys has become important in the automotive and maritime sectors and has the potential application for high strength aerospace alloys due to lighter and cheaper structures. Tungsten Inert Gas (TIG) welding is one of the frequently used methods, primarily because of its optimum weld quality, minimum distortion, and operativity in all positions.

Figure 1 shows the schematic of the TIG welding process. In welding fixed pipe as shown in Figure 2, the excessive arc current yields a meltdown of metals; in contrast, an insufficient arc current produces imperfect welding. The difficulty in controlling the arc welding process is in how to detect the weld pool geometrical features, such as weld bead width and penetration. Previous research using the welding system with a plain mirror to reflect the backside image of the molten pool has been successfully conducted to weld aluminum pipe (Baskoro, et al., 2008; Baskoro, et al., 2009).

* Corresponding author's email: ario@eng.ui.ac.id, Tel. +62-21-7270032 Ext. 203, Fax. +62-21-7270033

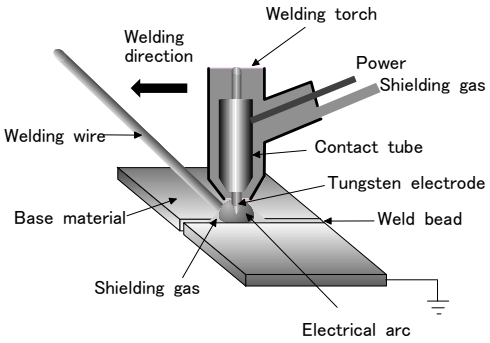

Figure 1 Schematic of TIG welding process

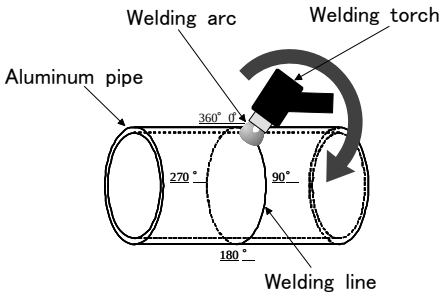

Figure 2 Schematic of pipe welding

In this study we propose a new method of monitoring of molten pool using omnidirectional vision-based molten pool monitoring using a hyperboloidal mirror and a CCD camera (Baskoro, et al., 2009; Baskoro, et al., 2009). However, compared to the detected stainless steel's image, the image of the aluminum molten pool has very low brightness. Therefore, a new technique of optimization in detecting the edge of the molten pool was proposed. The method, optimization using Particle Swarm Optimization (PSO), was compared with Genetic Algorithm (GA) used in a previous experiment (Baskoro, et al., 2009).

In this experiment, image processing algorithm was conducted by transforming the original image of the molten pool into a panoramic image. In application of the edge detection of the molten pool, a method for determining brightness range values for edge detection using PSO was proposed and compared with the GA method used in previous experiments (Baskoro, et al., 2009). Both search methods could potentially reduce both the computational cost and the error of detection. Next, the brightness range values were applied to the control system to obtain the performance of the image processing algorithm. The rest of this paper is organized as follows; the edge detection of the molten pool is described in Section 2. Later in Section 3, the experimental results are presented. Finally, section 4 provides a summary of the paper.

2. EDGE DETECTION OF MOLTEN POOL

2.1. Experiment Device

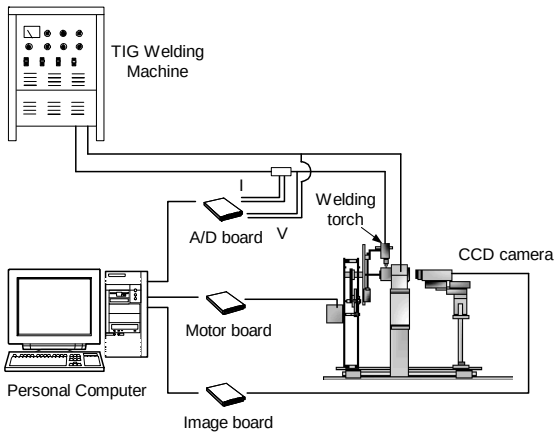

Figure 3 Welding experiment system

The experimental device used in this experiment is shown in Figure 3. The overall system consists of a circumferential welding system, a CCD camera and an image digitizer (256×220pixels, 8bit), a personal computer (CPU: 700MHz), stepping motors for the movement of the welding torch, arc current measurement equipment, a gearbox, and the TIG welding machine.

A CCD camera was used for monitoring the molten pool and sent the image to the personal computer through the image digitizer. The backside image of the molten pool was processed by the personal computer to detect the image parameter of the molten pool. Base metal used in this experiment was aluminum alloy pipe A6063S-T5. A pulsed TIG AC welding machine with square-wave current and pure argon shielding gas was used. The material properties and welding conditions are shown in Table 1.

Table 1 Material properties and welding conditions

Base metal	Al-6063S-T5
Diameter of pipe (mm)	37.8
Thickness of pipe (mm)	2.0
Density (g/cm^3)	2.69
Melting point (^{o}C)	615-655
Thermal conductivity (W/m.K at 25^{o}C)	209
Welding machine	AC
Electrode	2% Th-W (∅ 2.4 mm)
Nominal arc length (mm)	1.5
Welding current, I (A)	50 ~ 70
Welding speed, v (cm/min)	12 ~ 20
Shielding gas	100% Ar
Shielding gas, q (l/min)	8 ~ 15

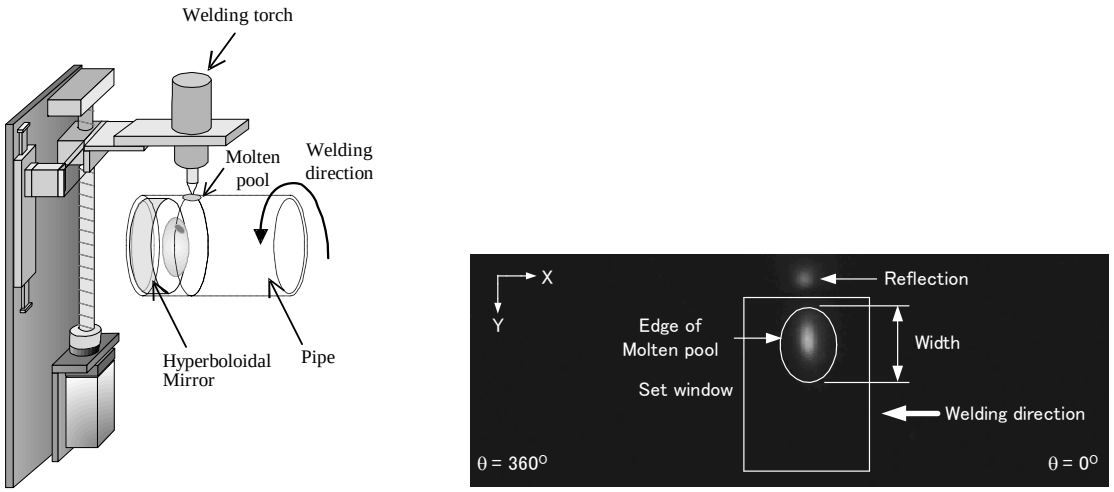

(a) Schematic of monitoring (b) Panoramic image of the molten pool

Figure 4 Monitoring of the molten pool

2.2. Monitoring of the Molten Pool

In order to capture the backside molten pool image, a hyperboloidal mirror was used to acquire the image reflected from the mirror. The schematic of the monitoring system is shown in Figure 4(a). The hyperboloidal mirror reflects the molten pool image into the CCD camera. Figure 4(b) presents the result after the transformation of the original image into a panoramic image (Baskoro, et al., 2009; Kim, et al., 2007).

A flowchart of the image processing algorithm is shown in Figure 5. Because of the low brightness of the aluminum's molten pool due to the low melting point, the stable and robust image processing algorithm had to be constructed. The focus of the optimization was on the histogram analysis process. In this step, the histogram analysis process was conducted.

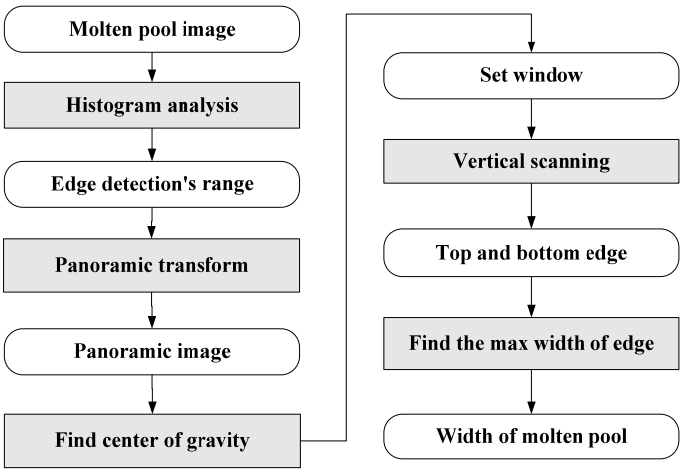

Figure 5 Flowchart of image processing

The frequency of the brightness value of the image, *f(i)*, the brightness average, g_{avg} and the accumulation of the percentage of brightness average, p_{avg} were obtained by Equations (1) and (2), respectively (Baskoro, et al., 2008).

$$g_{avg} = \frac{\sum_{i=0}^{i=255} \left(f(i) \times i \right)}{\sum_{i=0}^{i=255} i} \tag{1}$$

$$p_{avg} = \frac{\sum_{i=0}^{i=avg} f(i)}{\sum_{i=0}^{i=255} f(i)} \times 100\% \tag{2}$$

where:

$f(i)$ = the frequency of brightness at i.

By adding the percentage at brightness average, p_{avg}, with some values which are difference percentage of outer brightness (Δp_{out}) and difference percentage of inner brightness (Δp_{in}), the value of percentage of outer (p_{out}) and inner brightness (p_{in}) could be determined as shown in Equations (3) and (4), respectively.

$$p_{out} = p_{avg} + \Delta p_{out}(\%) \tag{3}$$

$$p_{in} = p_{avg} + \Delta p_{in}(\%) \tag{4}$$

Figure 6(a) illustrates the image of the molten pool. The edge of the molten pool is aligned between the outer and inner brightness. The cumulative percentage of brightness frequency is shown in Figure 6(b).

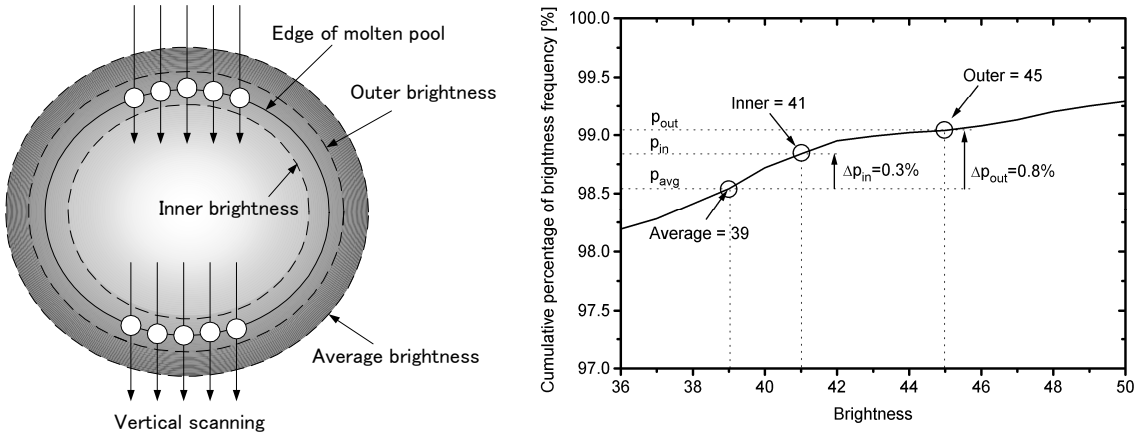

(a) Illustration image of molten pool (b) Inner and outer brightness frequency(θ=180^o)

Figure 6 Histogram analysis for edge detection

From Equations (3) and (4), we find the brightness of outer and inner, g_{out} and g_{in} as shown in Figure 6 (b). The range between g_{out} and g_{in} will be defined as the brightness range for determining the edge of the molten pool. Next, vertical scanning in set window was performed to find the edge. In this study, the values of p_{out} and p_{in} were optimized using PSO and GA to find the minimum error of detected width.

2.3. Particle Swarm Optimization and Genetic Algorithm

PSO was developed by Edward and Kennedy in 1995. The process behind the algorithm was inspired by the social behavior of animals, such as birds flocking or fish schooling. PSO is similar to the continuous GA in that it begins with a random population matrix. However, unlike the GA, PSO has no evolution operators such as crossover and mutation. The rows in the matrix, called particles, contain variable values and are not binary encoded. Each particle moves about the cost surface with velocity. The particles update their velocities and positions based on the local and global best solutions (Haupt & Haupt, 1998):

$$v_{m,n}^{new} = \omega \times v_{m,n}^{old} + \Gamma_1 \times r_1 \times \left(p_{m,n}^{local\ best} - p_{m,n}^{old}\right) + \Gamma_2 \times r_2 \times \left(p_{m,n}^{global\ best} - p_{m,n}^{old}\right) \tag{5}$$

$$p_{m,n}^{new} = p_{m,n}^{old} + v_{m,n}^{new} \tag{6}$$

where;

$v_{m,n}$: particle velocity
ω : inertia weight
$p_{m,n}$: particle variables
r_1, r_2 : independent uniform random numbers
$\Gamma_1 = \Gamma_2$: learning factors
$p_{m,n}^{local\ best}$: best local solution
$p_{m,n}^{global\ best}$: best global solution

The genetic algorithm (GA) is an optimization and search technique based on the principles of genetics and natural selection. GA encodes the decision variables (or input parameters) of the underlying problem into (solution) strings. Each string, called individual or chromosome, represents a candidate solution. Characters of the string are called genes. A fitness function is needed for differentiating between good and bad solutions. Three basic genetic operators, selection, crossover, and mutation, are applied to generate new individuals (Ahn, 2006; Haupt, 1998).

2.4. Edge Detection

In order to apply PSO or GA for edge detection, each particle in PSO of GA represents the percentages of outer (pout) and inner brightness (pin). The fitness function value, defined as error of edge detection, is calculated by the following equation,

$$f = \left| \left(1 - \frac{w_c}{w_t} \right) \times 100\% \right| \tag{7}$$

where w_c and w_t are the computed width and corresponding target of width, respectively. Therefore, the problem result is to minimize the problem. The dimensional search space for PSO and GA is limited to the percentage of brightness from 90% to 100% with which the brightness values of 25 – 255 were aligned. As shown in Figure 7, based on their fitness, agents in the population are guided by the position and speed of PSO or Eq. (5) and (6) and also by genetic operators of GA. New p_{out} and p_{in} are generated by PSO or GA. The algorithm is stopped when satisfied by two conditions: 1) Minimum error of edge detection – the detection value of the best agent is below the given threshold ($1x10^{-3}$%), or 2) the maximum iteration number is reached.

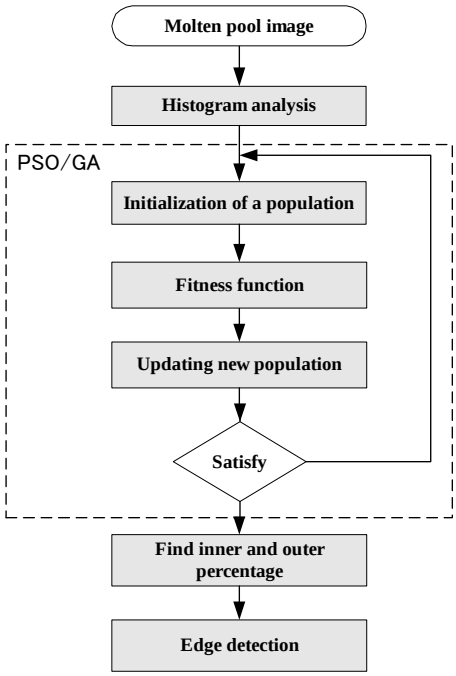

Figure 7 Flowchart of edge detection of molten pool using PSO or GA

3. EXPERIMENT RESULTS

3.1. Image Processing Optimization

This subsection presents experiment results of image processing optimization on edge detection using the proposed method. The experiment's conditions:

- Original image size is 256 x 220 pixels
- Panoramic image size is 512 x 186 pixels
- Maximum set window size is 150 x 100 pixels

PSO condition:

- $\Gamma_1 = \Gamma_2$ = learning factors = 2

GA condition:

- Crossover operator is single point crossover
- Mutation rate is 0.15
- Fraction of the population is 0.5

Figure 8 shows the comparison of experiment results using PSO and GA at $\theta = 270^o$ and iteration of 10. Both PSO and GA can determine the low error of detection. However, GA needs a higher population to get the same error as PSO. Figure 9 presents graphics of population size when the cost of fitness function in maximum iteration is 10. The PSO achieves the lower cost at 3.38%, faster than GA. PSO also reaches the minimum cost at the population size of 16, lower than GA which is 36. From the optimization process, the result shows that PSO and GA can optimize the brightness range.

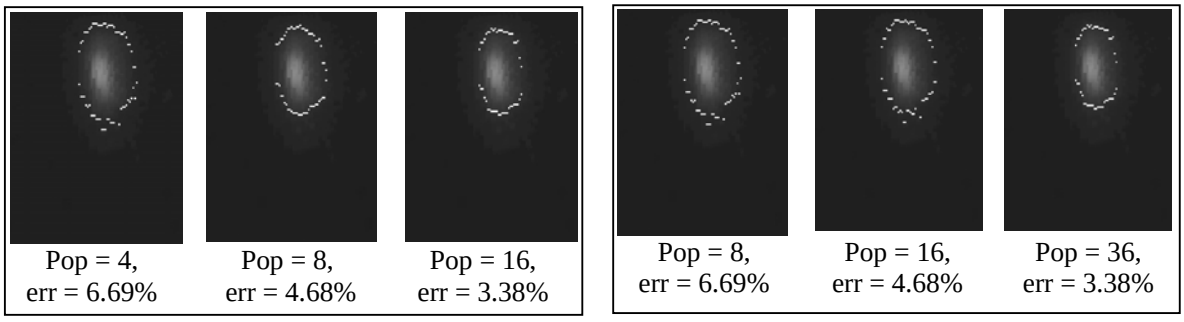

(a) PSO (b) GA

Figure 8 Edge detection of molten pool in set window using PSO and GA at $\theta = 270^o$ and iteration is 10

After optimizing 10 data of p_{out} and p_{in} generated by PSO, the values of Δp_{out} and Δp_{in} calculated from Eq. (3) and (4) were averaged. The average values of Δp_{out} and Δp_{out} from PSO were 0.14% and 0.79%, respectively. These values were compared with the average values of Δp_{out} and Δp_{out} from GA optimization and were 0.04% and 0.69%, respectively (Baskoro, et al., 2009). Both values were used for the proposed image processing algorithm.

Figure 10 shows the relation between measured back bead width and detected molten pool width. Image resolution was 0.093 mm/pixel. It is clearly seen that image processing algorithm using both PSO and GA optimization can detect the molten pool width with good approximation. PSO and GA achieved the RMSE of 1 mm and the standard deviation was 0.5 mm. The cause of the errors might come from the detected threshold values as the brightness range for scanning the edge of the molten pool. Very low brightness of the molten pool also generated poor detection of threshold values; therefore, the edge detection could be faulty.

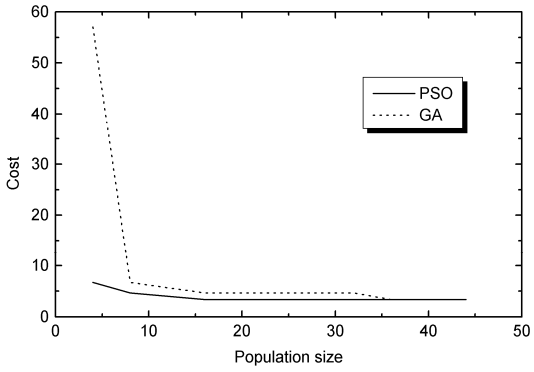

Figure 9 The population size vs the fitness function cost in maximum iteration number is 10

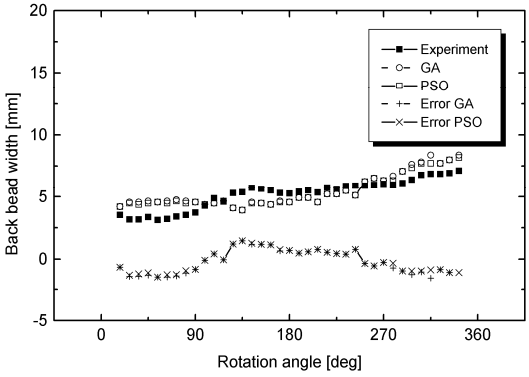

Figure 10 The result of measured back bead width from experiment, GA and PSO approximation, and both errors of detection

3.2. Fuzzy Control

This section presents an experiment with control using a fuzzy inference system. The welding process was conducted autogenously for 360^o of circumference and in a fixed position of pipe. The experiment with control was conducted using fuzzy inference system. The output of the image processing, which is the width of the molten pool, becomes the input of fuzzy control. The output of fuzzy control is the correction of the welding speed.

In this study, the proposed fuzzy control had two variables to be fuzzified. One was an error (e_n), which was the difference between back bead width (w_n) at the concerned time step (n) and the reference back bead width (w_r) which was set at 5 mm. The other variable was the change of an error, Δe_{n+1}. Three kinds of membership (N – Negative, Z – Zero, P – Positive) and triangular membership functions were used to fuzzify the inputs. Figure 11 (a), (b), (c) shows the membership functions and ranges for each fuzzy variable. Figure 11 (d) presents the decision table for the fuzzy control of welding speed (Baskoro, et al., 2008; Baskoro, et al., 2009).

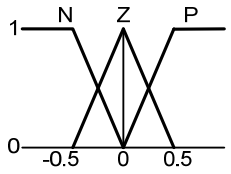

(a) Input: back bead width error, e [mm]

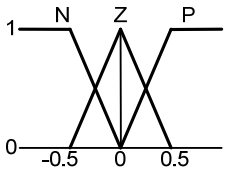

(b) Input: back bead width error deviation, Δe [mm]

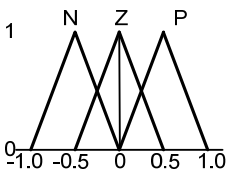

(c) Output: welding speed correction, Δv [cm/min]

Δe \ e	N	Z	P
N	N	N	Z
Z	N	Z	P
P	Z	P	P

(d) Decision table

Figure 11 Fuzzy sets and decision table for fuzzy control of welding speed

3.3. Results and Discussion

In the control experiment, to produce a stable arc condition, a constant welding speed of 7 cm/min at $\theta = 0^o$-45^o was used. Figure 12 shows the experiment results using control with PSO. The result of back bead width and welding speed using fuzzy controller is shown in Figure 12(a). It is shown that fuzzy control could determine the correction of welding speed to keep the back bead width in the target range of 5±1 mm. Compared with the results using GA optimization (Baskoro, et al., 2009), the result of back bead width and welding speed has also the same result which is the correction of welding speed has kept the back bead width in the

target range of 5±1 mm. The result of the experiment with control has an average error of 0.3 mm and a standard deviation of 0.4 mm. The results using PSO are lower than in GA, which has the average error of 0.3 mm and standard deviation of 0.6 mm. The back bead width increases slightly due to the starting speed. Back bead width is kept stable by maintaining the welding speed at around 8-12.5 cm/min. Back bead appearance is shown in Figure 12(b). In general, the proposed automatic welding system produced a sound weld of aluminum pipes by monitoring the backside image of molten pool using an omnidirectional camera.

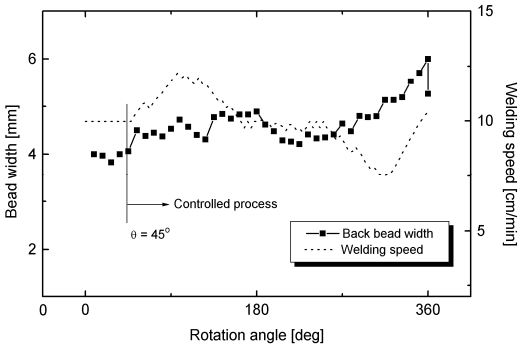

(a) Back bead width and welding speed

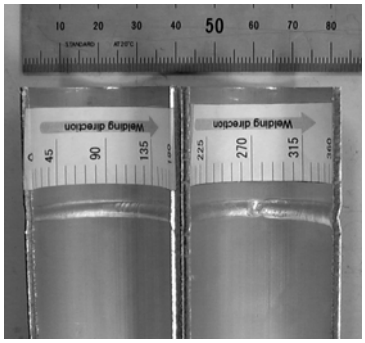

(b) Back bead appearance

Figure 12 Result of experiment with control using PSO

4. CONCLUSIONS

The conclusions of this paper are summarized as follows:

- This research proposes molten pool detection of fixed aluminum pipe welding using PSO as compared to using GA. The brightness range for edge detection was constructed using the percentage of outer brightness (p_{out}) and inner brightness (p_{in}).
- The experimental results show that the proposed method can detect the edge of the molten pool with minimum error, although PSO can reach minimum error faster than GA. The method can perform the optimization of brightness range, reducing the computational cost and time consumption.
- PSO optimized image processing algorithm was applied into the real time process using omnidirectional vision-based monitoring of the molten pool. From the experimental results using fuzzy inference system, image processing algorithm and the described control system are effective.

5. REFERENCES

Ahn, C.W., 2006. Advances in Evolutionary Algorithms: Theory, Design and Practice, *Springer-Verlag Heidelberg*, New York, USA.

Baskoro A. S., Kabutomori M., Suga Y., 2008. Automatic Welding System of Aluminum Pipe by Monitoring Backside Image of Molten Pool Using Vision Sensor, *Journal of Solid Mechanics and Materials Engineering, JSME*, Volume 2, Number 5, pp. 582-592.

Baskoro A. S., Masuda R., Kabutomori M., Suga Y., 2009. Welding Penetration Control for Aluminum Pipe Welding Using Omnidirectional Vision-based Monitoring of Molten Pool, *Quarterly Journal of the Japan Welding Society*, Volume 27, Number 2, pp.17-21

Baskoro, A.S., Masuda, R., Kabutomori, M., Suga, Y., 2009. An Application of Genetic Algorithm for Edge Detection of Molten Pool in Fixed Pipe Welding, *International Journal of Advanced Manufacturing Technology*, Volume 45, pp. 1104-1112.

Haupt R. L. & Haupt S.E., 1998. Practical Genetic Algorithms, 2nd Edition, *A John Wiley & Sons Inc. publication*, New Jersey, USA.

Kennedy J. & Eberhart R., 1995. Particle Swarm Optimization, *Proceedings of IEEE International Conference on Neural Networks*, p. 1942-1948.

Kim J., Muramatsu M., Murata Y., Suga Y., 2007. Omnidirectional Vision-Based Ego-Pose Estimation for an Autonomous In-pipe Mobile Robot, *Advanced Robotics*, Volume 21, Number 3-4, pp.441-460.